Acid-induced Aggregation and Gelation of Sodium Caseinate-Guar Gum Mixtures

María Eugenia Hidalgo . Manuel Fontana . Mirta Armendariz . Bibiana Riquelme . Jorge R. Wagner . Patricia Risso

María Eugenia Hidalgo (✉) . Manuel Fontana . Mirta Armendariz . Bibiana Riquelme . Patricia Risso
Departamento de Química-Física, Facultad de Ciencias Bioquímicas y Farmacéuticas, Universidad Nacional de Rosario (UNR), Suipacha 531 (2000) Rosario, Argentina
e-mail: maruhidalgo80@yahoo.com.ar

María Eugenia Hidalgo (✉) . Bibiana Riquelme . Patricia Risso
Instituto de Física Rosario (IFIR, CONICET-UNR), 27 de Febrero 210 Bis (2000) Rosario, Argentina

Jorge R. Wagner
Departamento de Ciencia y Tecnología, Universidad Nacional de Quilmes-CONICET, Roque Saénz Peña 352, (B1876BXD) Bernal, Buenos Aires, Argentina

Patricia Risso
Facultad de Ciencias Veterinarias, Universidad Nacional de Rosario (UNR), Ovidio Lagos y Ruta 33, (2170) Casilda, Argentina

Keywords: Sodium caseinate/guar gum acid gels . Thermodynamic incompatibility . Rheological properties . Microstructure . Experiment design

Abstract

The aim of this work was to study the formation of bovine sodium caseinate (NaCAS) acid gels induced by addition of glucono-δ-lactone (GDL) in the presence of guar gum (GG). At low biopolymer's concentrations, a one-phase system was observed, whereas at higher mixture concentrations two-phase systems were formed. Aggregation (at low NaCAS concentrations) and gelation (at high NaCAS concentrations) processes were analyzed through the use of full and fractional factorial experiment designs, using turbidimetric and rheological techniques. Finally, the gel images were obtained by confocal laser scanning microscopy and the images were analyzed. Results showed that at low NaCAS concentrations, the presence of GG affects the pH at which aggregation begins but was not significant for the time at which aggregation begins. On the other hand, at high NaCAS concentrations, the concentration of GG only affected significantly the elastic character of acid gels. As polysaccharide concentration increases, the gels obtained were weaker and with larger pores. Also, the formation of NaCAS droplet-shaped structures at certain biopolymer ratio was observed. The presence of GG affects both the rate of gelation and phase separation, which, in turn, determine the type of gel microstructure. Phase separation seems to occur prior to protein gelation because the protein gel network is discontinued, hindering the gel compactness and reducing gel strength. In summary, GG modifies NaCAS stabilization (self-association and phase separation) and the viscoelasticity and microstructure of NaCAS acid gels. The control of such processes and properties would allow obtaining mixture gels with different textures.

Introduction

Acid gelation of milk proteins is of relevance during the manufacture of dairy products such as yoghurt-like desserts. During bovine sodium caseinate (NaCAS) acidification, a gel structure is formed as a result of the dissociation and aggregation of caseins fractions [1-4]. Also, the use of glucono-δ-lactone (GDL) as acidulant enables different rates of acidification, depending on the temperature, the GDL concentration and the presence of cosolutes such as polysaccharides [5-8].

Many dairy food products contain both proteins and polysaccharides that may contribute to their structural and textural characteristics through their aggregation and gelling behavior. The overall stability and texture of colloidal food system depend not only on the functional properties of the individual ingredients, but also on the nature and strength of the protein-polysaccharide interactions [9-10]. The addition of polysaccharides to a protein suspension can result in phase separation into a polysaccharide-enriched and a protein-enriched phase if the polysaccharide concentration exceeds a certain concentration [11-12]. Phase separation is often due to a segregative interaction between these biopolymers because of thermodynamic incompatibility.

In order to have a better understanding of milk proteins – polysaccharide interactions during acidification process it is convenient to use a relatively simple model system containing only two biopolymers: NaCAS and an uncharged, non gelling and water-soluble galactomannan such as guar gum (GG). NaCAS is extensively used in the food industry because of its functional properties, such as emulsion and foam stabilizer and gel formation [2, 13-14]. GG could swell and dissolve readily in coldwater, producing a highly viscous solution even at low concentrations [15]. Therefore, GG is widely used as thickening, water holding and stabilizing agent [16].

Antonov et al. (1999) suggested that the dominant mechanism which controls compatibility of casein and GG in water, at low ionic strength, involves the creation of weak water-soluble electrostatic complexes [17]. In 2007, the same authors informed that the phase separation observed in moderately concentrated mixtures depended on ionic strength and not on the state of the protein [18]. Neirynck et al. (2007) have also reported the existence of phase separation in NaCAS-GG mixed systems [19]. Agbenorhevi and Kontogiorgos's studies (2010) revealed a phase-separated system with the GG domains surrounded by a continuous NaCAS phase [20]. Spyropoulos et al. (2010) informed that the addition of sugar in concentrations of up to 15 wt % initially increased the miscibility of the mixtures, but a further increase in the sugar content had the opposite effect, increasing the incompatibility between the polysaccharide and the protein macromolecules [21]. Long et al. (2012) informed that NaCAS solution showed a slightly shear-thinning behavior but tended to behave in a Newtonian way when GG was added, which implied that molecular interactions occurred between NaCAS and GG in the solution system [16].

On the other hand, Bourriot et al. (1999) investigated the properties of micellar casein-GG mixed systems. They reported a phase separation and postulated that the rheological behavior of this mixture is governed by a network of flocculated casein and the galactomannan-enriched phase would contribute to a much lesser extent to the rheology of the flocculated system [22-23].

Many studies on the acid gelation process of NaCAS have been carried out over the last decades for single model systems [2, 5-6] or complex systems [7, 24-26]. NaCAS/GG mixtures have been used in emulsions and foams [16, 19, 27], but acid gels of these components have not been studied. The aim of this work was to investigate the kinetic of the formation of NaCAS/GG acid gels as model systems of acid dairy desserts. The

91 microstructure and rheological properties of these acid gels and their relationship with
92 NaCAS-GG interactions were also studied.

93 ## Materials and Methods

94

95 ### Materials

96

97 Bovine sodium caseinate powder (NaCAS), glucono-δ-lactone (GDL), gum guar (GG),
98 tris(hydroxymethyl)aminomethane (Tris) and 1-8 aniline naphtalene sulfonate (ANS) were
99 purchased from Sigma-Aldrich Co. (Steinheim, Germany), and used without further
100 purification. HCl and NaOH were provided by Cicarelli SRL (San Lorenzo, Argentina).
101 NaCAS and GG aqueous stock solutions, 10 wt % and 1 wt % respectively, were
102 prepared from dissolution of powders in distilled water under magnetic stirring at room
103 temperature. For thermodynamic compatibility assays, these solutions were prepared in
104 buffer Tris HCl 10 mM pH 6.80. Protein concentration was determined by the Kuaye's
105 method [28].
106 For spectrofluorometric assays, an aqueous stock solution 6 mM of ANS was prepared,
107 and stored in the dark at 4 °C. Its concentration was determined by absorbance
108 measurements using a molar absorption coefficient of $\varepsilon = 4950\ M^{-1}cm^{-1}$ at 350 nm.

109

110 ### Phase Diagram

111

Binary solutions of NaCAS/GG were prepared by carefully mixing weighed amounts of NaCAS (10 wt %) and GG (1 wt %) in buffer Tris HCl at room temperature.

Phase diagrams (binodals) were obtained using the method proposed by Spyropoulos et al. [21]. Series of polysaccharide/protein aqueous solutions were carefully prepared so as to give rise to binary systems with, in one case, the same polysaccharide concentration but with protein concentrations ranging from 0 to 4 wt % and, in the other case, the same protein concentration but with polysaccharide concentrations ranging from 0 to 0.45 wt %. A total of two samples were taken from each of these binary solutions and kept in sealed cuvettes in a humidity chamber (35 ºC and 40% humidity) for 24 h. The occurrence of phase separation (or not) was verified by visual inspection. Polysaccharide and protein concentrations, in each of the prepared binary solutions, correspond to a single point on the phase diagram. Indeed, this approach provides a ‘‘map’’ of the transition from the single-phase to the two-phase region of the phase diagram and the binodal curve can then be obtained as the best-fit curve to the points situated on either side of the borderline. Data were adjusted to an exponential decay function as shown below:

$$[GG] = a\, e^{-b[NaCAS]} \tag{1}$$

where [GG] and [NaCAS] are GG and NaCAS concentrations, respectively.

Intrinsic fluorescence spectra

Aiming at detecting any spectral shift and/or changes in the relative intensity of fluorescence (FI), excitation and emission spectra of NaCAS 0.1 wt % in the absence or presence of different concentration of GG were obtained. Previously, the excitation wavelength (λ_{exc}) and the range of protein concentration with a negligible internal filter effect were determined. Samples (3 ml) for spectral analysis and FI measurements were poured into a fluorescence cuvette (1 cm path length) and placed into a cuvette holder maintained at 35 ºC. Values of FI (n = 3) were registered within the range of 300 to 400 nm using a λ_{exc} of 291 nm.

Surface hydrophobicity (S_0)

S_0 was estimated using the ammonium salt of amphiphilic ANS as a fluorescent probe [29], in an Aminco Bowman Series 2 spectrofluorometer (Thermo Fisher Scientific, USA). Measurements were carried out using λ_{exc} and emission wavelength (λ_{em}) set at 396 and 489 nm respectively, at constant temperature (35 ºC). Both wavelengths were obtained from emission and excitation spectra of protein-ANS mixtures.

Samples (3 ml) containing ANS 4 mM and different concentrations of NaCAS 0.1 wt % or NaCAS/GG mixtures (FI_b) as well as the intrinsic FI without ANS (FI_p) were determined (n = 3). The difference between FI_b and FI_p (ΔF) was calculated, and S_0 was obtained as the initial slope in the ΔF vs. protein concentration (wt %) plot.

Changes in average size and degree of compactness of particles by turbidimetry

Changes in the average size of particles were followed by the dependence of turbidity (τ) on wavelength (λ) of the suspensions, and determined as:

$$\beta = 4.2 + \frac{\partial \log \tau}{\partial \log \lambda} \quad (2)$$

The β parameter has a direct relationship with the average size of the particles, and can be used to detect and follow rapid size changes [30-31]. It is obtained from the slope of log τ vs. log λ plots, in the 450 to 650 nm range, where the absorption due to the protein chromophores is negligible, thus allowing τ estimation as absorbance in 400 to 800 nm range [32]. It has been shown that β, for a system of aggregating particles of the characteristics of NaCAS, tends, upon aggregation, towards an asymptotic value that can be considered as a fractal dimension (D_f) of the aggregates [30, 33]. τ was measured as absorbance (A) using a Spekol 1200 spectrophotometer (Analytikjena, Belgium), with a diode array detector. Determinations of β were the average of at least duplicate measurements.

Acid Aggregation

Kinetics of NaCAS 0.5 wt % and NaCAS/GG mixtures aggregation, induced by acidification with GDL, was analyzed by measuring τ in the range of 450 to 650 nm, as mentioned above. The amount of GDL added was calculated using the following relation (R):

$$R = \frac{GDL\ mass\ fraction}{NaCAS\ mass\ fraction} \quad (3)$$

Acidification was initiated by adding solid GDL to 6 g of samples. Absorption spectra and absorbance at 650 nm (A_{650nm}) were registered as a function of time until a maximum and constant A_{650nm} was reached; the decrease of pH was simultaneously measured. Assays were performed at least in duplicate. Values of β parameter were calculated as presented in the previous section. From β vs. time (t) and β vs. pH plots, the t at which the aggregation step begins (t_{ag}) and the pH value observed at the t_{ag} (pH_{ag}) were determined when a sharp increase in the value of β was observed [4].

Experimental Design

In order to analyze the data obtained during the study of NaCAS acid aggregation a full factorial design 2^3 was carried out, considering the following factors: amount of GDL (R), temperature (T) and GG concentration (C_{GG}), at two levels. Aggregation time (t_{ag}), aggregation pH (pH_{ag}) and D_f were the response variables studied.

The factors and interactions that were significant were analyzed by ANOVA tables. Using the corresponding model, the responses were adjusted. To visualize the behavior of the response variables, surfaces plots were performed for each situation.

Viscometry

The aggregation process is limited by diffusion, which depends on the medium viscosity (η). Therefore, it is important to determine the effect that the presence of the polysaccharide exerts on that property. The η was measured in triplicate, using a rotational LV Master (LVDV-III) Brookfield viscosimeter (Brookfield Engineering Laboratories, USA) with cone/plate geometry (CP-42), thermostatically controlled at 35 ºC and a shear rate of 3 rpm. The relative viscosity (η_r) was calculated as:

$$\eta_r = \frac{\eta}{\eta_0} \quad (4)$$

where η is the solution viscosity and η_0 is the solvent viscosity.

Rheological properties of acid gels - Experimental Design

Rheological properties of NaCAS samples, in the absence or presence of GG, were determined in a stress and strain controlled AR G2 model rheometer (TA Instruments, USA) using a cone geometry (diameter: 40 mm, cone angle: 2°, cone truncation: 55 mm) and a system of temperature control (19 and 50 ºC) with a recirculating bath (Julabo model ACW 100, Germany) connected to a Peltier plate. An amount of solid GDL according to a certain R (0.5 or 1) was added to initiate the acid gelation. Measurements were performed each 20.8 sec during 120-180 min with a constant oscillation stress of 0.1 Pa and a frequency of 0.1 Hz. The Lissajous figures at various times were plotted to ensure that the measurements of storage or elastic modulus (G') and loss or viscous modulus (G'') were always obtained within the linear viscoelastic region.

The G'-G" crossover times (t_{gel}) of acidified systems were considered as the gel times, since most studies of milk/caseinate gelation have adopted this criterion [6, 34]. The pH at t_{gel} was also determined considering the pH value at the G'-G" crossover (pH_{gel}). Also, the maximum storage modulus (G'_{max}) was determined. Measurements were performed at least in duplicate.

To evaluate the significance of the effects of independent variables T, R, C_{GG} and concentration of NaCAS (C_{NaCAS}) on the dependent variables t_{gel}, pH_{gel} and maximum elasticity of gel mesh (G'_{max}), a fractional factorial design 2^{4-1} was carried out. The factors and interactions that were significant were analyzed by ANOVA tables. Using the corresponding model, the responses were adjusted and, for each situation, surface plots were performed.

In order to analyze the effect that GG has on these rheological parameters, tests in the above conditions but in the absence of GG were also performed.

Confocal laser scanning microscopy (CSLM)

NaCAS (3 or 5 wt %) and NaCAS:GG mixtures (3 or 5 wt % : 0.05; 0.25; 0.45 wt %) were stained with Rhodamine B solution (2 mg L^{-1}). An adequate amount of GDL (R = 1) was added to initiate the gelation process. Aliquots of 200 μL were immediately placed in compartments of LAB-TEK II cells (Thermo Scientific, USA). The gelation process was performed in a bath at (19 ± 1) °C, keeping humidity controlled. Gels were observed with an 20x objective, without zoom and with 2x and 4x zoom, by using an inverted scan confocal microscope NIKON TE2000E (Nikon Instruments Inc., USA), with handheld

scanning, using 543 nm excitation He-Ne laser, 605-675 nm band emission. Acquired images were stored in tiff format for their further analysis.

The images were analyzed with PC software Image J v.1.48s. The plugin Bone J v.1.3.12 was applied [35] and the thickness of the background was calculated by Hildebrand and Ruegsegger [36].

Statistical Analysis

Data presented are average values ± standard deviations. Statistical analysis was performed with Sigma Plot 10.0, Minitab 16 and Design Expert 6 software. The relationship between variables was evaluated by correlation analysis, using Pearson correlation coefficient (p). Differences were considered statistically significant at $p < 0.05$ values. Small p-values imply that the effects (or coefficients) are much greater than their standard error [37].

Results and discussion

Thermodynamic compatibility of NaCAS/GG mixtures

In systems made up of protein and uncharged polysaccharides, as the system under study, the incompatibility between the biopolymers increases when the pH is higher than the isoelectric pH (pI) of the protein. However, at pH < pI protein aggregation results in gel formation [38]. The relative concentration of a biopolymer mixture is critical to the process of gelation. An increased concentration of macromolecule may improve the process, since the particles are closer to each other, facilitating the formation of aggregates and

261 contributing to the compactness of the structure [24, 39]. However, above a critical value,
262 thermodynamic incompatibility may occur with phase separation [40].
263
264 Figure 1
265
266 Figure 1 shows the results obtained for NaCAS/GG mixtures. From this graph it can be
267 concluded that NaCAS and GG have a limited compatibility. At low biopolymer
268 concentrations, a one-phase system was observed, whereas at higher mixture
269 concentrations, two-phase systems were predominant. This would indicate the existence of
270 segregative interactions which promote a lower NaCAS-rich phase and an upper GG-rich
271 phase. The compatibility curve was obtained by a mathematical adjustment using an
272 exponential decay function of two parameters, as suggested by Spyropoulos et al. (2010)
273 [21]:

$$[GG] = 5.42\, e^{-9.46[NaCAS]} \quad (5)$$

274 Other authors also observed phase separation but at higher NaCAS and GG
275 concentrations than those we reported [17, 19]. These authors worked at a pH similar but at
276 lower temperatures and obtained the phase diagrams only an hour after performing the
277 mixture of biopolymers. Although a system of two biopolymers is thermodynamically
278 unstable, phase separation may not be observed in the experimental period due to the
279 existence of a kinetic energy barrier associated with the restricted movement of the
280 molecules. If one or both biopolymers are highly viscous or form gels, the rate and extent

of phase separation may be severely delayed [41]. Therefore, it is possible that apparently monophasic system at first become biphasic system at longer times.

Despite the fact that Spyropoulos et al. (2010) also incubated NaCAS/GG mixtures for 24 h, they reported a higher miscibility region in the phase diagram [21]. This fact can be related to a difference in the incubation temperature. Their phase diagram was obtained at 20 ºC while the one presented in the current work was obtained at 35 ºC. An increase in temperature induces a decrease in mixture viscosity, therefore the rate and extent of the phase separation may be increased.

Conformational changes and surface hydrophobicity

Emission spectra of intrinsic fluorescence of NaCAS and mixtures at different NaCAS:GG ratios were analyzed (Figure 2). There was an increase in the FI for mixtures with lower proportions of GG (NaCAS:GG = 8:1) with respect to FI of NaCAS without GG. When the amount of GG increased, FI decreased. Although changes in emission peaks were not observed, this behavior is related to a change in the environment of the intrinsic protein fluorophores into a more polar media due to the presence of increasing concentrations of the polysaccharide [42].

Figure 2

According to the phase diagram, at the concentrations used in this experiment, the biopolymer blend is in a single phase state. Antonov et al. have hypothesized the existence of a small number of positively charged functional groups on GG molecules and the

formation of a complex due to the weak ionic interaction between the negatively charged NaCAS (pH > pI) and the positively charged GG [17]. If so, the NaCAS electrostatic stability decreases as the GG proportion increases, inducing the formation of NaCAS soluble aggregates. Farrell et al. have postulated that, during the formation of casein aggregates a compromise between tension and flexibility is established and a hydrophobic compression occurs; therefore, the aggregates remain open and highly hydrated [43]. So, the increase in the GG concentration would induce the formation of NaCAS soluble aggregates with a more open structure with the consequent exposure of protein fluorophores to a more polar media.

S_0 of the NaCAS was determined in the presence of different GG concentrations and the results are listed in Table 1. The presence of GG produced an initial increase of S_0 (when C_{GG} is 0.0125 wt %, NaCAS:GG ratio = 8:1) and then S_0 decreased as GG concentration increased. As explained above, this behavior might probably indicate a conformational change induced by the protein-polysaccharide interaction [17]. During the formation of NaCAS aggregates, the intermolecular interactions through hydrophobic regions are supposed to occur [43]. This fact would be related to the decrease in the ANS-binding sites.

Table 1

Acid aggregation of NaCAS/GG mixture

After addition of GDL, changes that lead to protein aggregation occurred. The β vs. t profiles (data not shown) showed the existence of two well defined stages. The first stage

328 was much slower, showing a decrease in the parameter β and a progressive increase in the τ
329 while the pH decreases. At pH near the isoelectric point of caseins (~ 4.6), when the
330 electrostatic stability is strongly affected due to a reduction in its net charge, a second stage
331 of aggregation occurs. This second stage was revealed by a sharp increase in τ and β until
332 the aggregates stop growing in size, which was evidenced by the invariability of these
333 parameters (values remain constant). These profiles suggest a slow dissociation of original
334 NaCAS aggregates to form a large number of small particles, which ultimately aggregate to
335 form bigger particles.

336 Table 2 shows the values of the independent variables assayed and the responses
337 obtained during the acid aggregation of NaCAS/GG mixture. Table 3 shows the
338 coefficients and p-values obtained in coded units for t_{ag}, pH_{ag} and D_f.

339

340 Table 2

341 Table 3

342

343 Linear terms of R and T were negative and statistically significant for t_{ag}; C_{GG} was not
344 significant (not considered). As mentioned above, t_{ag} depends on the rate of the first stage
345 of NaCAS dissociation during the acidification process. According to the results, the GG
346 would not affect the kinetics of the first stage.

347 Equation 6 contains the model for the variation of t_{ag}, as a function of the coded values,
348 obtained through a response surface and Figure 3A shows the response surface plot.

$$t_{ag} = 17.59 - 10.92\,T - 20.48\,R + 14.32\,R^2 + 11.41\,R\,T \qquad (6)$$

t_{ag} increased when R or T decreased but the effect of R was more significant. An increase in R induces an increment in the rate at which pH becomes lower and, therefore, this causes a decrease in the time required for NaCAS particles to become unstable and begin to aggregate. Moreover, the rise of T favors hydrophobic interactions involved in the aggregation process. Also, T increases the rate of hydrolysis of GDL and thus the rate at which pH becomes lower. Therefore, the kinetics of acid aggregation of NaCAS could be controlled by monitoring T and the amount of GDL added.

The linear terms of C_{GG} and T were statistically significant for pH_{ag}. Equation 7 contains the calculated coded mathematical model for the variation of pH_{ag}, obtained through response surface. Figure 3B shows the response surface plot obtained.

$$pH_{ag} = 4.67 - 0.42\,T - 0.36\,C_{GG} + 0.55\,T^2 - 0.41\,T\,C_{GG} \quad (7)$$

pH_{ag} decreased as T or C_{GG} increased. To start the aggregation process, it is necessary to remove the electrostatic repulsion due to the negative surface charges of NaCAS particles, and this is achieved by the binding of protons, which results from gluconic acid dissociation. Therefore, when T increases, it takes a higher concentration of protons to destabilize NaCAS electrostatically (lower pH). On the other hand, for a polyelectrolyte in aqueous solution, the relation between the variations of pH and T is known to fit the following equation:

$$\left(\frac{\partial\, pH}{\partial T}\right)_{\alpha,p} = -cte\frac{\Delta H_{d,i}}{\mathcal{R}T^2} \quad (8)$$

where α is the mole fraction of bound protons, p is the pressure, $\mathcal{R}$ is the gas constant and $\Delta H_{d,i}$ is the dissociation enthalpy of the amino acid residues [3]. Since pH increases when T decreases, the derivative is negative, and hence, $\Delta H_{d,i}$ is positive. Therefore, the protonation reaction is exothermic.

The changes of pH_{ag} due to the presence of GG suggested a stabilizing effect of the polysaccharide. As mentioned above, the interactions between NaCAS and GG would induce the formation of more open NaCAS aggregates, which would expose previously hidden protonable groups.

A change of R was not significant and this result confirms that the amount of GDL added only affects the kinetics of the aggregation process (t_{ag}).

Figure 3

None of the factors studied were significant for D_f ($p >> 0.05$). Therefore, the degree of compactness of the aggregates was not significantly modified by changes in T, C_{GG} or R in the ranges tested.

Rheological properties of NaCAS acid gels in the presence of GG

Rheological tests were performed on NaCAS concentrated aqueous solutions (3 and 5 wt %) in the absence and presence of GG. All curves obtained for variations of G' and G"

during the acidification process showed a slow stage where both moduli have very low values, indicating that blends mainly had a viscous behavior. This early stage was followed by a sharp increment in both moduli, especially of G', indicating that blends showed mainly an elastic behavior (data not shown). The same profiles were reported by Braga et al. (2006), and two stages in the gelation process promoted by GDL could be distinguished: the initial formation of the gel network and subsequent bond strengthening and/or local rearrangements which contribute to gel stiffness degree [6].

It is important to note that although the blends showed a phase separation at pH 6.8 (Figure 1) in the range of NaCAS and GG concentrations employed in the rheology assays, acid gels did not show macroscopic phase separation.

A fractional factorial design 2^{4-1} was applied to evaluate the significance of the effects of the independent variables T, R, C_{GG} and C_{NaCAS} on the responses t_{gel}, pH_{gel} and G'_{max}. Table 4 shows the coded and actual variable values and the responses obtained while Table 5 shows the coefficients and p-values obtained in coded units for t_{gel} and G'_{max}. None of the factors studied was significant for pH_{gel} ($p >> 0.05$).

Table 4

Table 5

Linear terms of C_{NaCAS}, R and T were negatively and statistically significant for t_{gel}; C_{GG} was not significant (not considered), indicating that GG would not affect the kinetics of the initial formation of gel network. Equation 9, which contains the calculated coded mathematical model for the variation of t_{gel}, was obtained by factorial adjustment.

$$t_{gel} = 16.52 - 1.36\,C_{NaCAS} - 5.83\,R - 10.37\,T + 4.49\,R\,T \quad (9)$$

Figure 4 shows the response surface plots obtained. Since plots of response surfaces are made using only two independent variables, the other factors remained constant.

An increase in C_{NaCAS} produced a decrease in t_{gel} as a consequence of a rise in effective collision probability during the formation of the first NaCAS aggregates.

t_{gel} decreased when R or T increased but the effect of T was more significant. When R increases, the rate at which the protonable groups of NaCAS are neutralized also increases, hence, t_{gel} decreases. Moreover, when T increases, the rate of the gelation process is faster and the hydrophobic interactions become more intense ($\Delta H > 0$). Also, T increases the rate of hydrolysis of GDL and thus the rate at which pH become lower; as a consequence, t_{gel} decreases.

Figure 4

None of the factors studied was significant for pH_{gel} ($p >> 0.05$). Therefore, the pH at t_{gel} was not significantly modified by changes in C_{NaCAS}, C_{GG}, T or R in the ranges tested, i.e. the electrostatic stability of NaCAS particles was not significantly modified by these factors.

Equation 10 shows the calculated coded mathematical model for the variation of G'_{max}, where T, C_{NaCAS}, C_{GG} and the interaction between both biopolymer concentrations were significant ($p < 0.05$).

$$\log G'_{máx} = 1.42 + 0.75 C_{NaCAS} - 0.15 C_{GG} - 0.66 T + 0.10 C_{NaCAS} C_{GG} \quad (10)$$

Figure 5 shows the response surface plots obtained. The higher C_{NaCAS}, the greater the elastic character (G'_{max}) of the gels formed due to higher amounts of protein particles that are involved in the formation of the gel mesh.

The change of T produces two opposite effects. On one hand, an increase in T promotes the establishment of hydrophobic interactions ($\Delta H > 0$) involved in the bond strengthening and/or local rearrangements of gel network. On the other hand, in protein/nonionic hydrocolloids systems, such as NaCAS/GG, pH only affects protein self-association since that hydrocolloid self-association and protein-hydrocolloid cross-association play a minor role [44]. Incompatibility is favored under conditions that promote biopolymer self-association, such as pH values near the protein pI [45-46]. An increase in T also favors casein self-association due to hydrophobic interactions that participate in this self-association process [47]. Moreover, an increment of T promotes a decrease in t_{gel}. As a result, the rearrangements of the interactions into the gel network are limited. Gels which take longer to form would be more compact and therefore more elastic. According to equation 10, the predominant effects would be the ones mentioned above.

Finally, the elastic character of gels decreases as GG concentration increases. As mentioned above, at higher concentrations of GG, phase separation due to thermodynamic incompatibility between both biopolymers occurs. The C_{GG} and C_{NaCAS} used in the rheological assays correspond to the zone of phase separation in the phase diagram (Figure 1). This thermodynamic incompatibility might hinder the gelation process and might

promote the formation of weaker gels. The interaction between C_{NaCAS} and C_{GG} factors will be analyzed by CSLM assays.

Figure 5

Microstructure of NaCAS acid gels in the presence of GG by CSLM

Figure 6 shows the images of NaCAS 3 and 5 wt % in the absence or presence of 0.05, 0.25 or 0.45 wt % of GG after the addition of GDL (R 1 and T 19 ºC).

Figure 6

As observed in the top row, in the absence or in the presence of 0.05 wt % of GG, NaCAS 3 wt % formed a continuous protein gel matrix, where the dark zones represent the pores or interstices and the red ones the NaCAS network. There was no significant difference in the average pore size obtained in these samples (data not shown). On the other hand, in the presence of 0.25 and 0.45 wt % of GG, at the same C_{NaCAS} (3 wt %), droplet-shaped structures were observed. In this case, the protein phase is compressed into spheres with an average diameter of 4–8 μm. Therefore, at these higher C_{GG}, the mixed NaCAS/GG gel microstructure is inverted from a protein continuous network to protein droplet-shaped structures in an aqueous phase concentration. This behavior is in agreement with the decrease of G'_{max} values for NaCAS 3 wt % acid gels in the presence of 0.25 and 0.45 wt % of GG (Table 4).

Other authors have reported that casein micelles-GG systems show this type of microstructure with caseins concentrated in spherical droplets [22, 48]. On the other hand, Pacek et al. (2000), in NaCAS/Na-alginate aqueous systems, have determined that droplet-shaped structures resulting from phase separation that to the naked eye appear to be homogeneous aqueous–aqueous dispersions [49]. Also, Rediguieri et al. (2007) informed that caseinate-pectin mixtures consist of caseinate-rich droplets in a pectin-rich continuous phase. It seems that pectin diffuses into the droplets and adsorbs onto micellar caseinates and stabilizes them [50]. It is important to note that all those studies were made on NaCAS/polysaccharide aqueous dispersions at pH far further away from the NaCAS pI. We have not seen reports about the observation of these droplet-shaped structures in NaCAS/polysaccharides mixed acid gels.

On the other hand, de Jong and van de Velde (2007) reported a phase inversion in mixed whey protein isolates/guar gum cold-set gels, obtained by lowering the pH with GDL. These authors informed that the microstructure of these gels result from the competition between the protein gel formation and the phase separation process between protein and polysaccharide [40].

The images of the microstructure of NaCAS 5 wt % acid gels obtained with and without different C_{GG} could be observed in the bottom row of Figure 6. As can be observed, the network formed in the absence of GG was more homogeneous with very little pores. On the other hand, in the presence of 0.05 and 0.25 wt % of GG, the network became less homogeneous with higher pores. This behavior was more significant as C_{GG} increased. In the presence of 0.45 wt % of GG, the continuous protein network was disrupted by the enlarging volume fraction of the polysaccharide phase, and the phase inversion seems to

occur at a higher polysaccharide concentration. These results are in agreement with the rheology behavior mentioned above (Table 4).

Figure 7 shows the pore size distribution of NaCAS-GG mixture gels corresponding to the images in the bottom row of Figure 6 (NaCAS 5 wt %). It can be observed that, in the absence of GG (Figure 7A), most of the pores have the smallest size (0.28 μm). As C_{GG} increases, the pore size distribution changes, increasing the amount of pores with larger size. The size of 50 % of the pores was 0.47 μm for 0.05 wt % GG (Figure 7B), 9.86 μm for 0.25 wt % GG (Figure 7C) and 34.74 μm for 0.45 wt % GG (Figure 7D). This pore size increment is in agreement with the decrease of the elastic character of mixed gels. Inclusive, at highest C_{GG}, the samples resembles a viscous liquid.

Bourriot et al. (1999) postulated that the rheological behavior of casein micelles-GG mixtures is governed by a network of flocculated casein and the GG enriched phase contributing to a much lesser extent to the rheology of the flocculated system [22]. de Jong et al. (2009) concluded that, in the presence of polysaccharides, the gelation induces phase separation between protein aggregates and polysaccharide molecules [38]. Incompatibility is directly correlated to protein self-association, which is strongest at the pI and leads to reenlargement of the two-phase region [44]. The competition between the ongoing gelation process and the phase separation results in the final microstructure. This competition occurs in a short time frame after which the microstructure is frozen [38]. The microstructure of the resulting gel will depend on the relative rate of these two processes. Such microstructure also depends on the rate of acidification, the relative concentrations of both biopolymers and the extent of the interactions that lead to protein self-association.

Conclusions

The addition of GG to aqueous solutions of NaCAS induced protein conformational changes due to weaker interactions between both biopolymers at low concentrations and thermodynamic incompatibility with segregative phase separation at higher concentrations.

The experimental design allowed us to evaluate the significance of the effects of temperature, GDL and NaCAS mass fraction ratio and concentration of GG on the kinetics of NaCAS aggregation induced by GDL, and the degree of compactness of the aggregates formed. It was observed that the time at which the aggregation begins (t_{ag}) depended on both, the amount of GDL added and the temperature, the first variable effect being the most significant. The pH value necessary to destabilize NaCAS particles depended on temperature and the concentration of GG, the latter related to the variation of the amount of protein protonable groups due to conformational changes. The degree of compactness of the aggregates estimated through fractal dimension was independent of all factors studied.

During the gelation process, the model equations allow us to evaluate and to predict the behavior of the dependent variables as a function of the different factors analyzed. It was observed that the concentration of GG only affected significantly the elastic character of acid gels (G'_{max}). As polysaccharide concentration increases, the gels obtained were weaker and with large pores, as shown in the images of gel microstructure obtained by CSLM. Also, the formation of NaCAS droplet-shaped structures at certain biopolymers ratio was observed. The presence of GG affects both the rate of gelation and phase separation, which, in turn, determine the type of gel microstructure. Above a given concentration of GG, the protein gel network is discontinued, hindering the gel compactness and reducing gel strength. In this case, it seems that phase separation occurs prior to protein gelation.

Further studies about these microstructures could be performed in order to deepen the understanding on the conditions in which these structures are formed and to clarify the interactions that take place.

In summary, GG modifies NaCAS stabilization (self-association and phase separation) and the viscoelasticity and microstructure of NaCAS acid gels. Thus, these findings may be used to obtain mixture gels with different textures according to the relative concentration of NaCAS and GG and other conditions of the process.

Acknowledgements

This work was supported by grants from Universidad Nacional de Rosario (UNR), Argentina. We thank the English Area of Facultad de Ciencias Bioquímicas y Farmacéuticas-UNR, for the language correction of the manuscript and Julia Lombardi for the advice during the image analysis. María Eugenia Hidalgo is research fellow of Consejo Nacional de Investigaciones Científicas y Técnicas (CONICET), Argentina.

Figure captions

Fig. 1. Approach used for the determination of the phase diagrams for NaCAS/GG systems after 24 h at 35°C. Key: (●) two-phase samples; (○) one-phase clear solution; (◍) one-phase turbid solution

Fig. 2. Emission spectra of intrinsic fluorescence (FI) of NaCAS and NaCAS:GG mixtures at different ratios: (—) without GG; (— —) 8:1; (---) 6:1; (— · —) 2:1; y (— · · —) 1:1.5. NaCAS 0.1 wt %, T 35 ºC.

Fig. 3. Response surface plots: (A) t_{ag} (min) as a function of GDL mass fraction/NaCAS mass fraction ratio (R) and T (ºC); (B) pH_{ag} as a function of guar gum concentration (C_{GG}: wt %) and T (ºC).

Fig. 4. Response surface plot for t_{gel} (min): (A) t_{gel} as a function of C_{NaCAS} (wt %) and T (°C); (B) t_{gel} as a function of C_{NaCAS} (wt %) and R; (C) t_{gel} as a function of R and T (ºC).

Fig. 5. Response surface plots of log G'_{max} (Pa): (A) log G'_{max} as a function of C_{NaCAS} (wt %) and T (ºC); (B) log G'_{max} as a function of C_{GG} (wt %) and T (ºC); (C) log G'_{max} as a function of C_{GG} (wt %) and C_{NaCAS} (wt %).

Fig. 6. Microstructure of acid NaCAS/GG gels with different concentration of NaCAS and GG obtained by CSLM after addition of GDL. Top row: C_{NaCAS} 3 wt %, bottom row: C_{NaCAS} 5 wt %. Objective 20x without or with 4x zoom, C_{GG} = 0, 0.05, 0.25 or 0.45 wt %, R 1 and 19°C.

Fig. 7. Pore size distribution of NaCAS gels without and with different C_{GG}: (A) NaCAS without GG, (B) NaCAS with GG 0.05 wt %, (C) NaCAS with GG 0.25 wt % and (D) NaCAS with GG 0.45 wt %. C_{NaCAS} = 5 wt %, R 1 and T 19 °C.

References

1. J.A. Lucey, M. Tamehana, H. Singh, P.A. Munro, Food Res. Int. **31**, 147 (1998)
2. B.T. O'Kennedy, J.S. Mounsey, F. Murphy, E. Duggan, P.M. Kelly, Int. Dairy J. **16**, 1132 (2006)
3. C.G. de Kruif, J. Colloid Interf. Sci. **185**, 19 (1997)
4. M.E. Hidalgo, M.A. Mancilla Canales, C.R. Nespolo, A.D. Reggiardo, E.M. Alvarez, J.R. Wagner, P.H. Risso, *Comparative study of bovine and ovine caseinate aggregation processes: Calcium-induced aggregation and acid aggregation*, in *Protein Aggregation*, ed. by D.A. Stein (Nova Publishers, Hauppauge, NY, 2011), p. 199
5. K.P. Takeuchi,R.L. Cunha, Dairy Science Technology **88**, 667 (2008)
6. A.L.M. Braga, M. Menossi, R.L. Cunha, Int. Dairy J. **16**, 389 (2006)
7. A.L.M. Braga,R.L. Cunha, Food Hydrocolloid. **18**, 977 (2004)

8. M.E. Hidalgo, B. Riquelme, E.M. Alvarez, J.R. Wagner, P. Risso, *Acid-Induced Aggregation and Gelation of Bovine Sodium Caseinate-Carboxymethylcellulose Mixtures*, in *Food Industrial Processes- Methods and Equipment*, ed. by B. Valdez, R. Zlatev, M. Schorr (InTech Publisher, Rijeka, Croatia, 2012), p. 75
9. E. Dickinson, *Emulsion stabilization by polysaccharides and protein-polysaccharides complexes*, in *Food polysaccharides and their applications*, ed. by A.M. Stephen (Marcel Dekker Inc., New York, 1995), p. 501
10. E. Dickinson, Trends in Food Science & Technology **9**, 347 (1998)
11. V.Y. Grinberg,V.B. Tolstoguzov, Food Hydrocolloid. **11**, 145 (1997)
12. V.B. Tolstoguzov, Food Hydrocolloid. **4**, 429 (1991)
13. M.P. Ennis,M.D. Mulvihill, *Milk proteins*. (Woodhead Publishing Limited and CRC Press LLC, Cork, 2000)
14. A. HadjSadok, A. Pitkowski, T. Nicolai, L. Benyahia, N. Moulai-Mostefa, Food Hydrocolloid. **22**, 1460 (2008)
15. H. Maier, M. Anderson, C. Karl, K. Magnuson, R.L. Whistler, *Guar, locust bean gum, tara, and fenugreek gums*, in *Industrial gums*, ed. by R.L.W.J.N.B. (Eds.) (Academic Press, New York, 1993), p. 181
16. Z. Long, Q. Zhao, T. Liu, W. Kuang, J. Xu, M. Zhao, Food Res. Int. **49**, 545 (2012)
17. Y.A. Antonov, J. Lefebvre, J.-L. Doublier, Journal of Applied Polymer Science **71**, 471 (1999)
18. Y. Antonov, J. Lefebvre, J.-L. Doublier, Polym. Bull. **58**, 723 (2007)
19. N. Neirynck, K. Van lent, K. Dewettinck, P. Van der Meeren, Food Hydrocolloid. **21**, 862 (2007)
20. J.K. Agbenorhevi,V. Kontogiorgos, Carbohydrate Polymers **81**, 849 (2010)
21. F. Spyropoulos, A. Portsch, I.T. Norton, Food Hydrocolloid. **24**, 217 (2010)
22. S. Bourriot, C. Garnier, J.-L. Doublier, Food Hydrocolloid. **13**, 43 (1999)
23. S. Bourriot, C. Garnier, J.-L. Doublier, Int. Dairy J. **9**, 353 (1999)
24. C.S.F. Picone,R.L. da Cunha, Food Hydrocolloid. **24**, 502 (2010)
25. K.O. Ribeiro, M.I. Rodrigues, E. Sabadini, R.L. Cunha, Food Hydrocolloid. **18**, 71 (2004)
26. M.W.W. Koh, L. Matia Merino, E. Dickinson, Food Hydrocolloid. **16**, 619 (2002)
27. D.J. Walsh, K. Russell, R.J. FitzGerald, Food Res. Int. **41**, 43 (2008)
28. A.Y. Kuaye, Food Chem. **49**, 207 (1994)
29. A. Kato,S. Nakai, Biochim. Biophys. Acta **624**, 13 (1980)
30. P. Risso, V. Relling, M. Armesto, M. Pires, C. Gatti, Colloid Polym. Sci. **285**, 809 (2007)
31. M.A. Mancilla Canales, M.E. Hidalgo, P.H. Risso, E.M. Alvarez, J Chem Eng Data **55**, 2550 (2010)
32. R.D. Camerini-Otero,L.A. Day, Biopolymers **17**, 2241 (1978)
33. D.S. Horne, Faraday Discuss. Chem. Soc. **83**, 259 (1987)
34. S. Curcio, D. Gabriele, V. Giordano, V. Calabrò, B. de Cindio, G. Iorio, Rheol. Acta **40**, 154 (2001)
35. M. Doube, M.M. Kłosowski, I. Arganda-Carreras, F.P. Cordelières, R.P. Dougherty, J.S. Jackson, B. Schmid, J.R. Hutchinson, S.J. Shefelbine, Bone **47**, 1076 (2010)
36. T. Hildebrand,P. Rüegsegger, Journal of Microscopy **185**, 67 (1997)
37. J.F.M. Burkert, F. Maugeri, M.I. Rodrigues, Bioresource Technol. **91**, 77 (2004)

38. S. de Jong, H.J. Klok, F. van de Velde, Food Hydrocolloid. **23**, 755 (2009)
39. F. Yamamoto,R.L. Cunha, Carbohydrate Polymers **68**, 517 (2007)
40. S. de Jong,F. van de Velde, Food Hydrocolloid. **21**, 1172 (2007)
41. C.M. Bryant,D.J. McClements, Food Hydrocolloid. **14**, 383 (2000)
42. J.R. Lakowicz, *Principles of fluorescence spectroscopy*. (Plenum Press, USA, 1986)
43. H.M. Farrell, P.X. Qi, E.M. Brown, P.H. Cooke, M.H. Tunick, E.D. Wickham, J.J. Unruh, J. Dairy Sci. **85**, 459 (2002)
44. A. Syrbe, W.J. Bauer, H. Klostermeyer, Int. Dairy J. **8**, 179 (1998)
45. C.G. de Kruif,R. Tuinier, Food Hydrocolloid. **15**, 555 (2001)
46. J.L. Doublier, C. Garnier, D. Renard, C. Sanchez, Curr. Opin. Colloid Interface Sci. **5**, 202 (2000)
47. P. Risso, D. Borraccetti, C. Araujo, M. Hidalgo, C. Gatti, Colloid Polym. Sci. **286**, 1369 (2008)
48. P.W. de Bont, G.M.P. van Kempen, R. Vreeker, Food Hydrocolloid. **16**, 127 (2002)
49. A.W. Pacek, P. Ding, A.W. Nienow, M. Wedd, Carbohydrate Polymers **42**, 401 (2000)
50. C.F. Rediguieri, O. de Freitas, M.P. Lettinga, R. Tuinier, Biomacromolecules **8**, 3345 (2007)

661 **Figure 1**

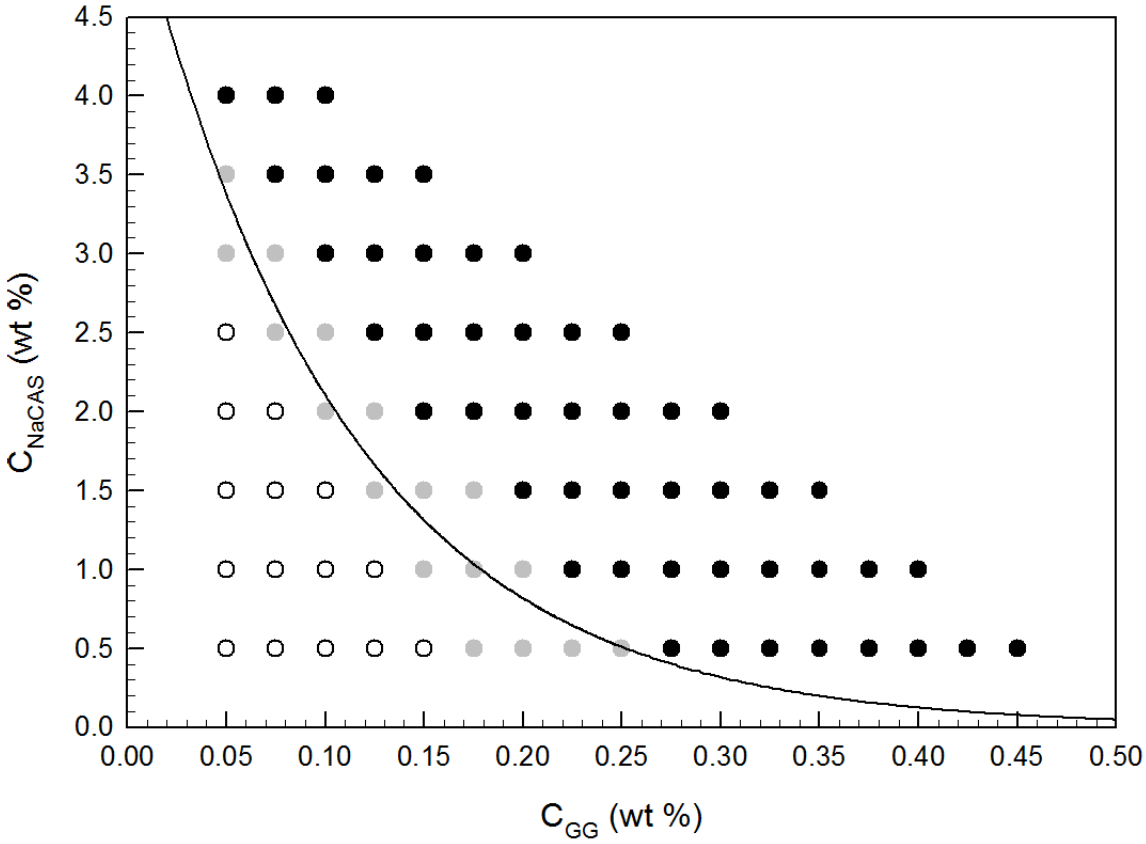

662

663 Fig. 1. Approach used for the determination of the phase diagrams for NaCAS/GG systems
664 after 24 h at 35°C. Key: (●) two-phase samples; (○) one-phase clear solution; (●) one-phase
665 turbid solution
666

667 **Figure 2**

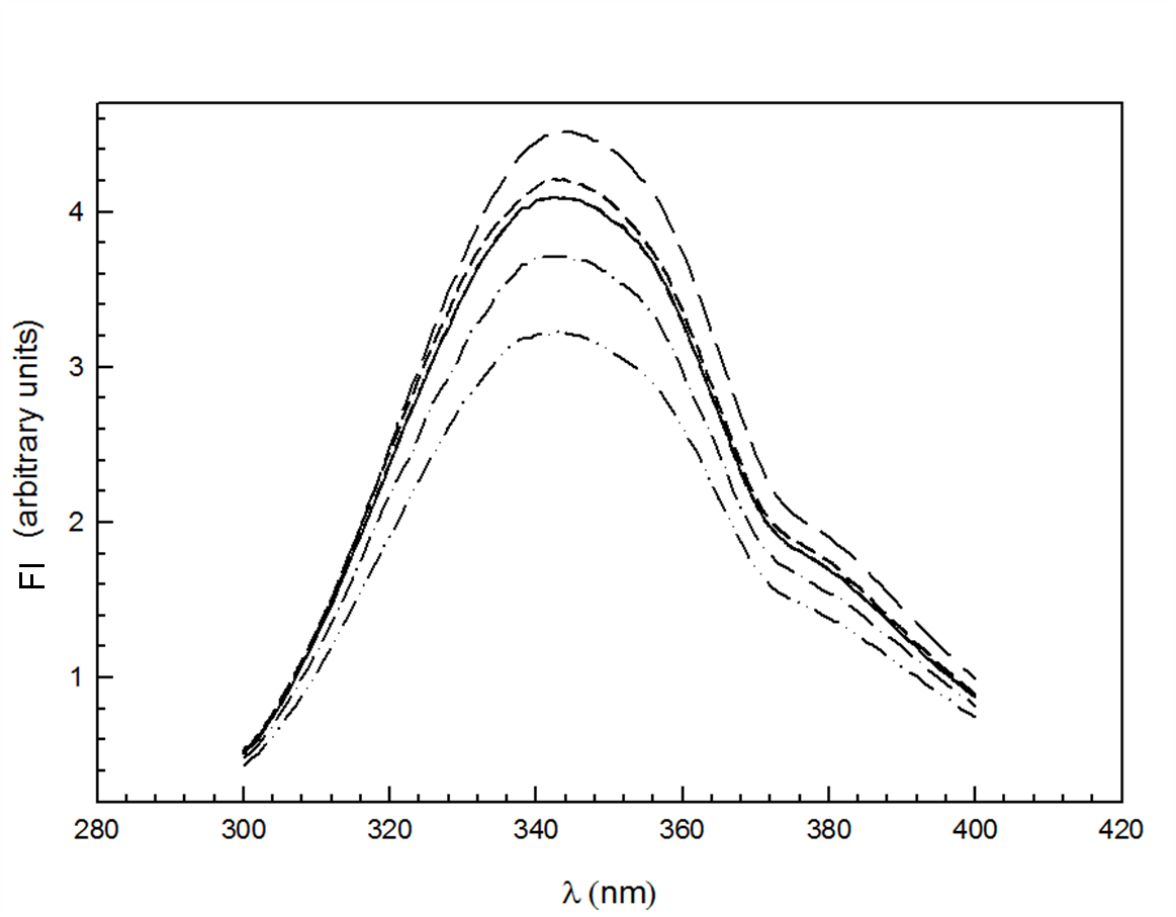

668

669 Fig. 2. Emission spectra of intrinsic fluorescence (FI) of NaCAS and NaCAS:GG mixtures
670 at different ratios: (—) without GG; (— —) 8:1; (---) 6:1; (— · —) 2:1; y (— · · —) 1:1.5.
671 NaCAS 0.1 wt %, T 35 ºC.
672

673 **Figure 3**

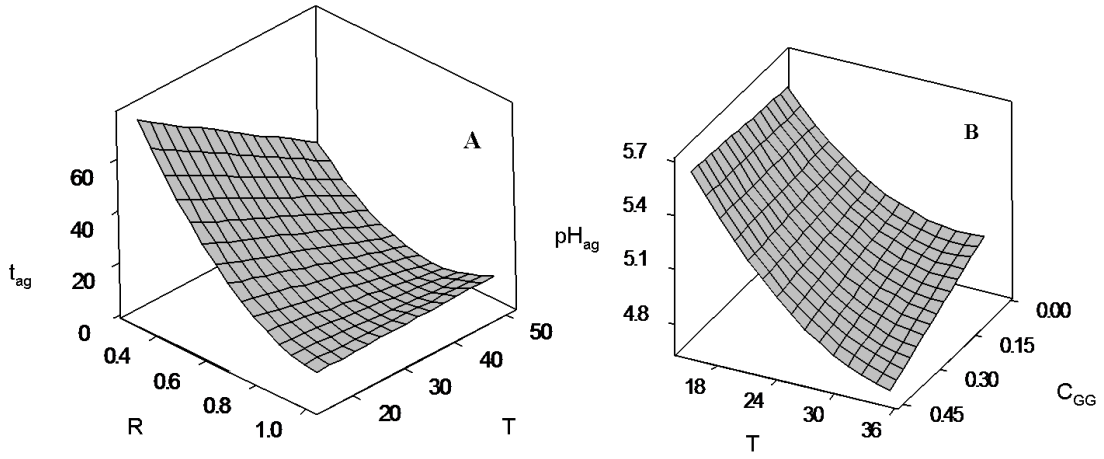

674

675 Fig. 3. Response surface plots: (A) t_{ag} (min) as a function of GDL mass fraction/NaCAS
676 mass fraction ratio (R) and T (ºC); (B) pH_{ag} as a function of guar gum concentration (C_{GG}:
677 wt %) and T (ºC).
678

679 **Figure 4**

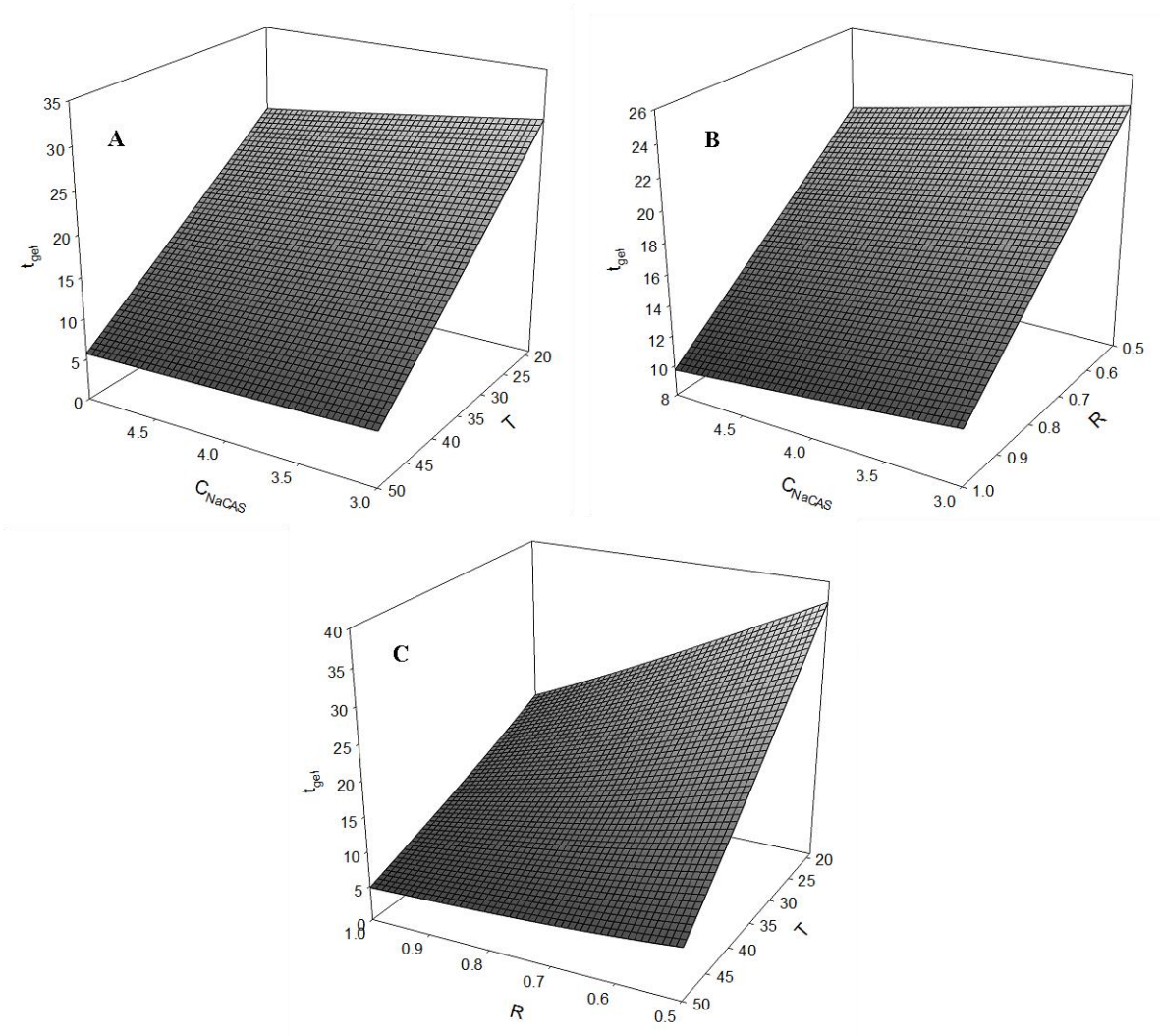

680

681 Fig. 4. Response surface plot for t_{gel} (min): (A) t_{gel} as a function of C_{NaCAS} (wt %) and T
682 (°C); (B) t_{gel} as a function of C_{NaCAS} (wt %) and R; (C) t_{gel} as a function of R and T (ºC).

683 **Figure 5**

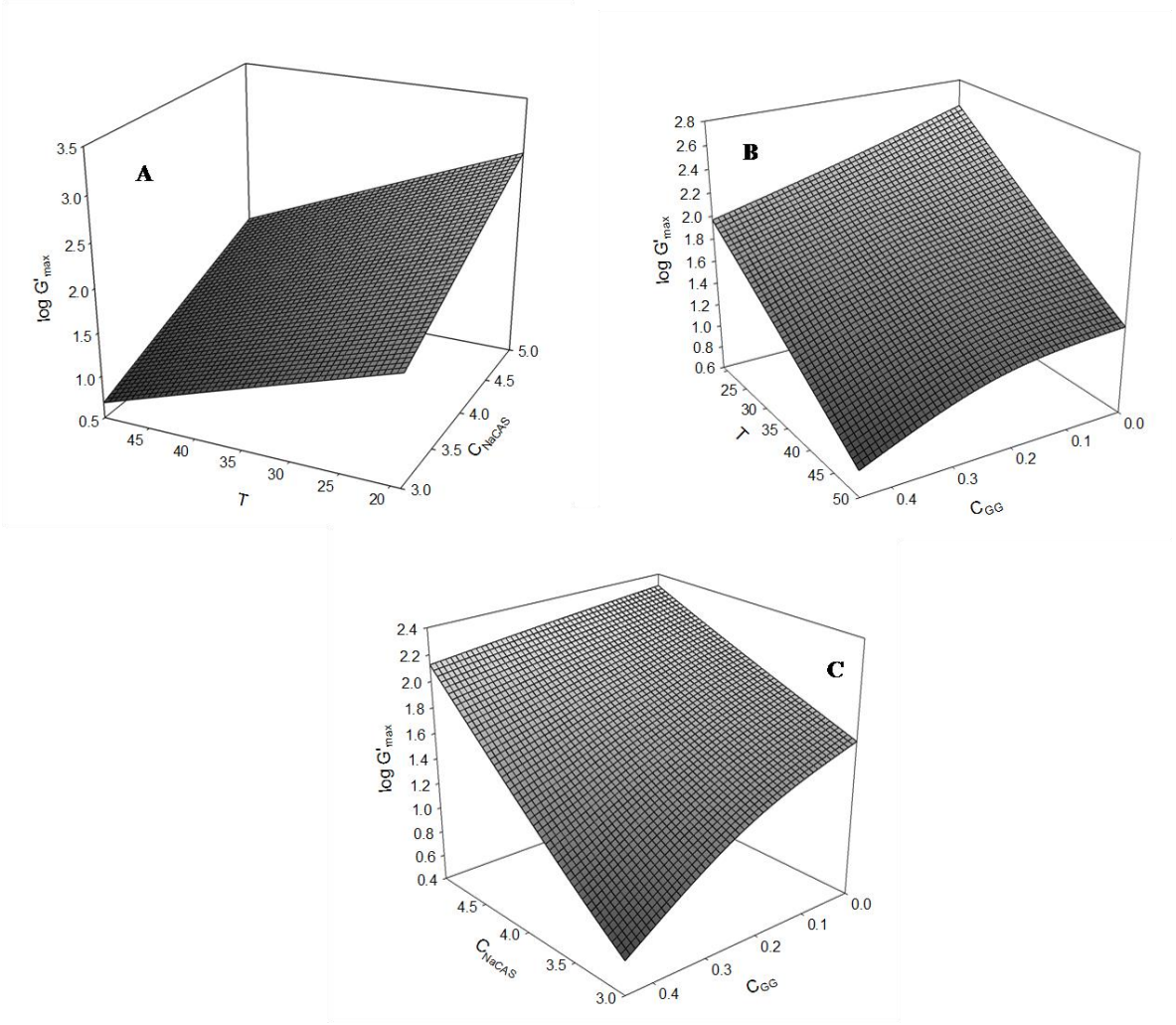

684

685 Fig. 5. Response surface plots of log G'_{max} (Pa): (A) log G'_{max} as a function of C_{NaCAS} (wt
686 %) and T (ºC); (B) log G'_{max} as a function of C_{GG} (wt %) and T (ºC); (C) log G'_{max} as a
687 function of C_{GG} (wt %) and C_{NaCAS} (wt %).

688 **Figure 6**

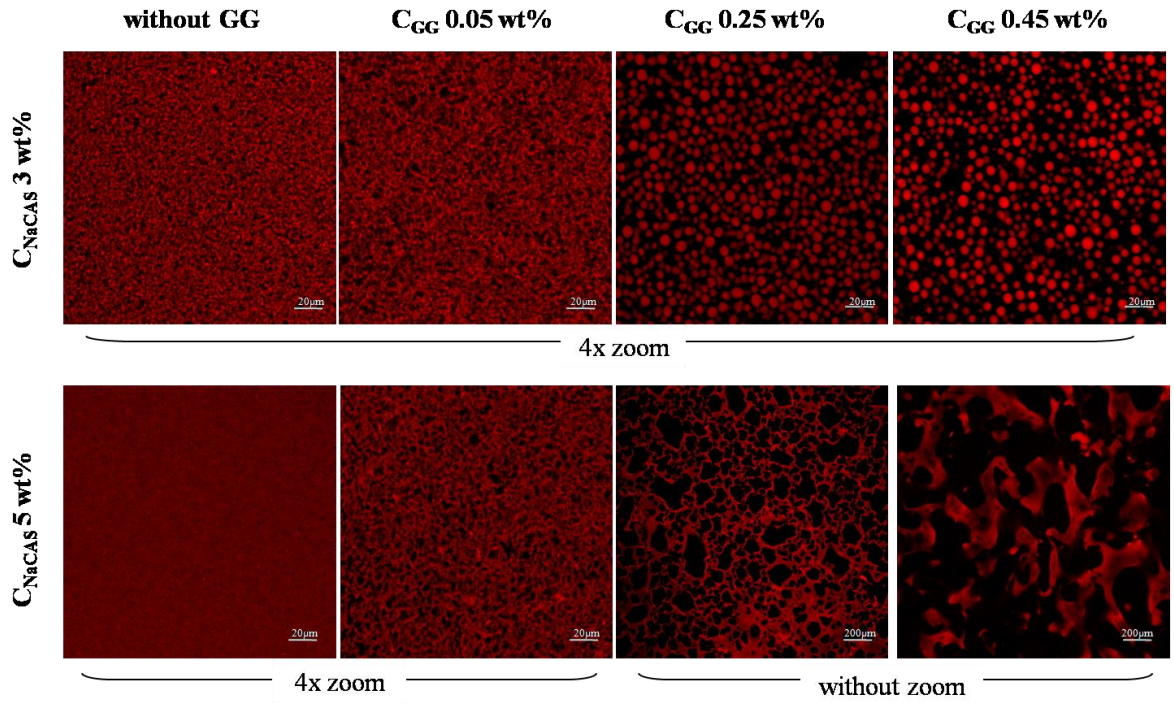

689

690 Fig. 6. Microstructure of acid NaCAS/GG gels with different concentration of NaCAS and
691 GG obtained by CSLM after addition of GDL. Top row: C_{NaCAS} 3 wt %, bottom row:
692 C_{NaCAS} 5 wt %. Objective 20x without or with 4x zoom, C_{GG} = 0, 0.05, 0.25 or 0.45 wt %,
693 R 1 and 19°C.

694 **Figure 7**

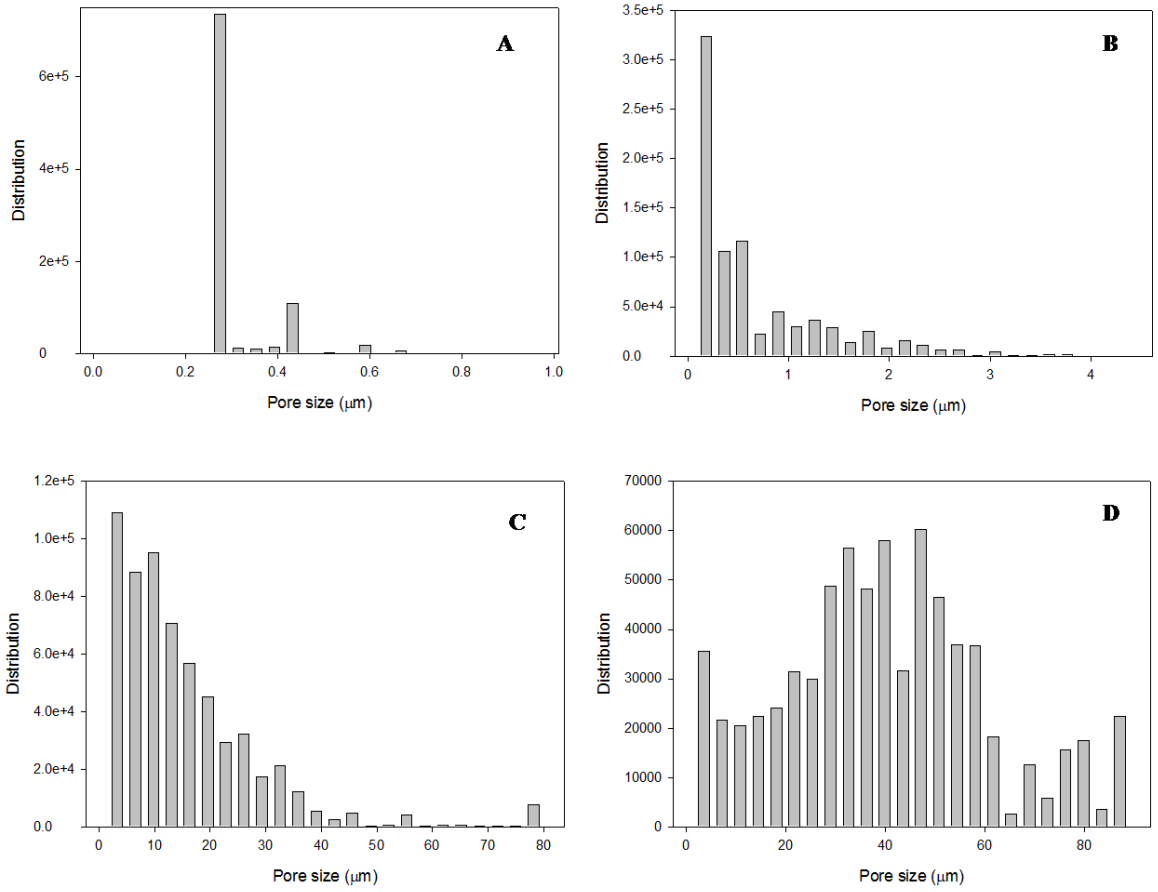

695

696 Fig. 7. Pore size distribution of NaCAS gels without and with different C_{GG}: (A) NaCAS
697 without GG, (B) NaCAS with GG 0.05 wt %, (C) NaCAS with GG 0.25 wt % and (D)
698 NaCAS with GG 0.45 wt %. C_{NaCAS} = 5 wt %, R 1 and T 19 °C.

Table 1

S_0 values of NaCAS in the presence of different concentrations of GG (C_{GG}) at 35ºC.

NaCAS:GG ratios (g/g)[a]	S_0 ($\%^{-1}$) ± 0.2[b]
1:0	60.7
8:1	144.2
4:1	72.6
2:1	50.6
1:1	33.4
1:1.5	51.2

[a] NaCAS concentration (C_{NaCAS}): 0.1 wt %
[b] Mean value ± standard deviation ($p < 0.05$)

Table 2

Aggregation times (t_{ag}), aggregation pH (pH_{ag}) and fractal dimensions (D_f) as function of the coded values for guar gum concentrations (C_{GG}), temperature (T) and GDL mass fraction/NaCAS mass fraction ratio (R) used in the experimental design, with the respective real values (C_{NaCAS}: 0.5 wt %)

Independent variables			Responses					
			t_{ag} (min) ± 0.2		pH_{ag} ± 0.02		D_f ± 0.001	
C_{GG} (wt %)	T (°C)	R	Original	Duplicate	Original	Duplicate	Original	Duplicate
0.05 (-1)	35 (+1)	1 (+1)	7.0	8.0	4.62	5.00	4.062	4.005
0.25 (0)	35 (+1)	1 (+1)	10.5	10.5	4.73	4.84	3.433	4.063
0.45 (+1)	35 (+1)	1 (+1)	9.0	10.0	4.70	4.23	3.908	3.149
0.05 (-1)	35 (+1)	0.7 (0)	13.0	13.0	5.11	5.11	4.044	4.060
0.25 (0)	35 (+1)	0.7 (0)	12.5	12.5	5.16	5.10	3.946	3.976
0.45 (+1)	35 (+1)	0.7 (0)	13.0	12.5	4.66	4.83	3.932	4.083
0.05 (-1)	35 (+1)	0.35 (-1)	54.0	48.0	4.99	5.15	3.844	4.050
0.25 (0)	35 (+1)	0.35 (-1)	48.0	56.0	4.99	4.98	3.927	4.017
0.45 (+1)	35 (+1)	0.35 (-1)	38.5	36.0	4.27	4.94	4.003	4.113
0.05 (-1)	25 (0)	1 (+1)	13.5	14.0	4.87	4.91	3.957	4.105
0.25 (0)	25 (0)	1 (+1)	13.5	13.5	5.10	5.09	4.011	4.103
0.45 (+1)	25 (0)	1 (+1)	13.0	15.0	4.74	4.76	4.175	4.136
0.05 (-1)	25 (0)	0.7 (0)	19.0	20.5	5.06	5.11	4.055	4.070
0.25 (0)	25 (0)	0.7 (0)	30.0	23.0	4.58	5.02	4.020	4.045
0.45 (+1)	25 (0)	0.7 (0)	22.0	21.5	5.13	5.13	4.039	3.979
0.05 (-1)	25 (0)	0.35 (-1)	52.0	52.0	5.29	5.29	4.062	4.064
0.25 (0)	25 (0)	0.35 (-1)	58.5	54.0	5.17	5.29	3.950	4.023
0.45 (+1)	25 (0)	0.35 (-1)	92.0	90.0	5.18	5.20	3.783	3.886
0.05 (-1)	15 (-1)	1 (+1)	9.5	10.5	5.51	5.66	4.110	4.080
0.25 (0)	15 (-1)	1 (+1)	11.8	10.8	5.21	5.48	4.056	4.035
0.45 (+1)	15 (-1)	1 (+1)	10.8	13.5	5.48	5.63	4.035	4.025
0.05 (-1)	15 (-1)	0.7 (0)	17.0	18.0	5.74	5.39	4.055	4.091
0.25 (0)	15 (-1)	0.7 (0)	17.5	25.5	5.44	5.72	4.110	4.070
0.45 (+1)	15 (-1)	0.7 (0)	21.5	21.0	6.15	5.87	4.050	4.084
0.05 (-1)	15 (-1)	0.35 (-1)	59.5	54.0	5.70	5.79	4.070	4.019
0.25 (0)	15 (-1)	0.35 (-1)	61.4	60.0	5.68	5.80	3.916	3.979
0.45 (+1)	15 (-1)	0.35 (-1)	133.7	132.5	5.28	5.39	3.785	3.932

Table 3

Analysis of the coefficients and p-values, obtained in coded units, of the responses t_{ag}, pH_{ag} and D_f.

	t_{ag}		pH_{ag}		D_f	
Factor	Coefficient	p-value	Coefficient	p-value	Coefficient	p-value
Constant	17.59	— [b]	4.67	— [b]	3.98	— [b]
C_{GG} (L)	-	— [a]	-0.36	0.005	-	— [a]
R (L)	-20.48	— [b]	-	— [a]	-	— [a]
T (L)	-10.92	— [b]	-0.42	— [b]	-	— [a]
C_{GG}*C_{GG} (Q)	-	— [a]	-	— [a]	-	— [a]
T*T (Q)	-	— [a]	0.55	— [b]	-	— [a]
R*R (Q)	14.32	— [b]	-	— [a]	-	— [a]
C_{GG}*T	-	— [a]	-0.41	— [b]	-	— [a]
C_{GG}*R	-	— [a]	-	— [a]	-	— [a]
R*T	11.41	— [b]	-	— [a]	-	— [a]
		r^2 = 83.67%		r^2 = 67.78%		r^2 = 89.00%

L = linear effect
Q = quadratic effect
[a] Not significant ($p >> 0.05$)
[b] Significant ($p << 0.05$)

Table 4

Gelation times (t_{gel}), gelation pH (pH_{gel}) and maximum elastic modulus (G'_{max}) as function of the coded values for sodium caseinate concentrations (C_{NaCAS}), guar gum concentrations (C_{GG}), temperature (T) and GDL mass fraction/NaCAS mass fraction ratio (R) used in the experimental design, with the respective real values.

Independent variables				Responses					
				t_{gel} (min) ± 0.2		pH_{gel} ± 0.02		G'_{max} (Pa) ± 0.01	
C_{NaCAS} (wt %)	C_{GG} (wt %)	R	T (°C)	Original	Duplicate	Original	Duplicate	Original	Duplicate
3 (-1)	0 (-1)	1 (+1)	19 (-1)	18.4	18.7	4.74	4.80	171.10	176.50
3 (-1)	0 (-1)	0.5 (-1)	19 (-1)	42.0	40.4	4.87	4.95	260.00	284.00
3 (-1)	0.45 (+0.8)	1 (+1)	19 (-1)	16.8	16.9	4.74	4.76	16.87	12.46
3 (-1)	0.25 (0)	0.5 (-1)	19 (-1)	41.1	38.9	4.88	4.88	16.89	17.78
5 (+1)	0 (-1)	1 (+1)	19 (-1)	16.7	16.7	4.70	4.56	541.80	567.70
5 (+1)	0 (-1)	0.5 (-1)	19 (-1)	37.3	35.5	4.62	4.57	726.70	716.40
5 (+1)	0.45 (+0.8)	0.5 (-1)	19 (-1)	31.6	30.9	4.91	4.94	506.70	657.20
5 (+1)	0.25 (0)	1 (+1)	19 (-1)	15.2	13.0	4.84	4.51	1603.00	1550.00
3 (-1)	0 (-1)	1 (+1)	50 (+1)	4.1	4.0	4.92	4.97	3.89	4.34
3 (-1)	0 (-1)	0.5 (-1)	50 (+1)	6.6	6.7	5.46	5.25	19.47	16.34
3 (-1)	0.25 (0)	1 (+1)	50 (+1)	7.3	7.1	3.99	4.01	0.55	0.50
3 (-1)	0.45 (+0.8)	0.5 (-1)	50 (+1)	8.6	8.5	4.80	4.75	1.49	1.50
5 (+1)	0 (-1)	1 (+1)	50 (+1)	3.8	-	4.92	-	45.13	46.30
5 (+1)	0 (-1)	0.5 (-1)	50 (+1)	7.4	-	4.94	-	89.72	93.54
5 (+1)	0.45 (+0.8)	1 (+1)	50 (+1)	4.0	4.5	4.65	4.43	38.54	22.94
5 (+1)	0.25 (0)	0.5 (-1)	50 (+1)	7.4	7.4	4.93	4.90	16.57	17.02

Table 5

Analysis of the coefficients and p-values obtained in coded units, of the responses t_{gel} and G'_{max}. None of the factors studied was significant for pH_{gel} ($p >> 0.05$).

	t_{gel}		G'_{max}	
Factor	Coefficient	p-value	Coefficient	p-value
Constant	16.52	— [b]	1.42	— [b]
C_{NaCAS} (L)	-1.36	— [b]	0.75	— [b]
C_{GG} (L)	-	— [a]	-0.14	— [b]
R (L)	-5.83	— [b]	-	— [a]
T (L)	-10.37	— [b]	-0.66	— [b]
C_{NaCAS}*C_{NaCAS} (Q)	-	— [a]	-	— [a]
C_{GG}*C_{GG} (Q)	-	— [a]	-	— [a]
R*R (Q)	-	— [a]	-	— [a]
T*T (Q)	-	— [a]	-	— [a]
C_{NaCAS}*C_{GG}	-	— [a]	0.10	— [b]
C_{NaCAS}*R	-	— [a]	-	— [a]
C_{NaCAS}*T	-	— [a]	-	— [a]
C_{GG}*R	-	— [a]	-	— [a]
C_{GG}*T	-	— [a]	-	— [a]
R*T	4.49	— [b]	-	— [a]
		r^2 = 97.30%		r^2 = 91.91%

L = linear effect
Q = quadratic effect
[a] Not significant ($p >> 0.05$)
[b] Significant ($p << 0.05$)